

Synthesis and Crystal Structure of $\text{Na}_3\text{V}(\text{SO}_4)_3$. Spectroscopic Characterization of $\text{Na}_3\text{V}(\text{SO}_4)_3$ and $\text{NaV}(\text{SO}_4)_2$

Soghomon Boghosian,^{*a} Rasmus Fehrmann^b and Kurt Nielsen^c

^aInstitute of Chemical Engineering and High Temperature Chemical Processes (ICE/HT-FORTH) and Department of Chemical Engineering, University of Patras, GR-26500 Patras, Greece, ^bChemistry Department A, The Technical University of Denmark, DK-2800 Lyngby, Denmark and ^cChemistry Department B, The Technical University of Denmark, DK-2800 Lyngby, Denmark

Boghosian, S., Fehrmann, R. and Nielsen, K., 1994. Synthesis and Crystal Structure of $\text{Na}_3\text{V}(\text{SO}_4)_3$, Spectroscopic Characterization of $\text{Na}_3\text{V}(\text{SO}_4)_3$ and $\text{NaV}(\text{SO}_4)_2$. – Acta Chem. Scand. 48: 724–731 © Acta Chemica Scandinavica 1994.

Dark green crystals of the compound $\text{Na}_3\text{V}(\text{SO}_4)_3$ suitable for X-ray structure determination were synthesized by dissolution of V_2O_5 in NaHSO_4 melt at 420°C under an $\text{SO}_2(\text{g})$ atmosphere. Slow cooling of the solution from 420 to 320°C over a period of one week gave a large number of small $\text{Na}_3\text{V}(\text{SO}_4)_3$ crystals. The compound crystallizes in the rhombohedral (hexagonal) space group $R\bar{3}$ with $a = b = 13.439(1)$, $c = 9.091(1)$ Å and $Z = 6$. It contains two independent almost perfect VO_6 octahedra (within which equal V–O bond lengths are found) linked by three identical bridging sulfate groups, as an infinite $-\text{V}-(\text{SO}_4)_3-\text{V}-$ chain parallel to the c -axis. All oxygens coordinated to vanadium belong to the significantly distorted equivalent sulfate groups, which contain four different types of oxygen. The infrared and Raman spectra of polycrystalline $\text{Na}_3\text{V}(\text{SO}_4)_3$ and $\text{NaV}(\text{SO}_4)_2$ have been recorded and interpreted. The severe distortion of the sulfate groups within $\text{Na}_3\text{V}(\text{SO}_4)_3$ leads to a more complicated pattern of the vibrational spectra [i.e. IR activity of $\nu_1(\text{SO}_4^{2-})$ and extensive splitting of $\nu_3(\text{SO}_4^{2-})$ in the IR and Raman spectra] compared to $\text{NaV}(\text{SO}_4)_2$. Above 1500 cm^{-1} the Raman spectra, particularly at lower temperatures, exhibit broad features which are interpreted as electronic Raman transitions between the ${}^3\text{E}_g$ and ${}^3\text{A}_g$ split levels of the ${}^3\text{T}_{1g}$ (${}^3\text{F}$) ground state of $\text{V}^{3+}(\text{d}^2)$ in octahedral oxide fields.

The molten system $\text{V}_2\text{O}_5/\text{MHSO}_4/\text{M}_2\text{S}_2\text{O}_7$ ($\text{M} = \text{K}$, Na and/or Cs) in contact with $\text{SO}_2/\text{O}_2/\text{SO}_3/\text{N}_2$ at 400 – 600°C represents a realistic model of the working industrial SO_2 oxidation catalyst¹ when water is present in the synthesis gas. Therefore, investigations of the chemistry of this system are considered essential for the understanding of this important process. Commercial alkali-promoted V_2O_5 catalysts contain mainly potassium as the promoter, together with small amounts of sodium. Recently, catalysts containing also cesium have been developed. At temperatures typically lower than 440°C the commercial catalysts undergo deactivation, and the influence of the type and amount of promoters on catalyst activity is well recognized.¹ Precipitation of V^{4+} (mainly) and V^{3+} crystalline compounds has been shown to be the reason for the activity loss during SO_2 oxidation in V_2O_5 – $\text{M}_2\text{S}_2\text{O}_7$ melts.² In particular, the compounds $\text{K}_4(\text{VO})_3(\text{SO}_4)_5$, $\text{KV}(\text{SO}_4)_2$, $\text{Na}_2\text{VO}(\text{SO}_4)_2$, $\text{NaV}(\text{SO}_4)_2$, $\text{Cs}_2(\text{VO})_2(\text{SO}_4)_3$ and $\text{CsV}(\text{SO}_4)_2$ have been identified as

deactivation products² and characterized by X-ray and spectroscopic methods.^{3–8} Furthermore an *in situ* ESR spectroscopic investigation on a working commercial catalyst has shown⁹ that the V^{4+} compound $\text{K}_4(\text{VO})_3(\text{SO}_4)_5$ is indeed formed during catalyst deactivation.

The present work concerns the crystal structure and the spectroscopic characterization of a new V^{3+} compound, $\text{Na}_3\text{V}(\text{SO}_4)_3$, which was discovered unexpectedly while attempting to synthesize $\text{NaV}(\text{SO}_4)_2$ from the molten-salt–gas system $\text{NaHSO}_4/\text{V}_2\text{O}_5$ – SO_2 . The infrared and Raman spectra of $\text{NaV}(\text{SO}_4)_2$ are also presented.

Experimental

Synthesis of green crystalline $\text{Na}_3\text{V}(\text{SO}_4)_3$. The compound was prepared by equilibrating an NaHSO_4 – V_2O_5 molten mixture with SO_2 in a pyrex ampoule. The NaHSO_4 used was from Fluka (> 99.5% pure) and was dried by heating under vacuum at 100°C for 2 h. The non-hygroscopic

* To whom correspondence should be addressed.

V₂O₅, Cerac, pure (99.9%), was used without further purification. The purity of SO₂ (Matheson/Union Carbide) was better than 98.5%. All handling of chemicals took place in a N₂-filled glove-box with a controlled water vapor content not exceeding 5 ppm.

Approximately 3 g of a NaHSO₄-V₂O₅ mixture with a molar ratio Na/V = 16 [i.e. mole fraction of V₂O₅, $X(\text{V}_2\text{O}_5) \approx 0.059$] were added into a 50 cm³ ampoule, which was then connected to a vacuum line and evacuated. Gaseous SO₂ was introduced at a pressure of 1.25 atm (at room temperature), and the ampoule was then sealed by keeping the lower part (containing the powderous chemicals and the liquified SO₂) immersed in liquid nitrogen.

The NaHSO₄-V₂O₅ molten-salt-gas mixture was equilibrated for several hours at 420°C inside a double quartz-walled transparent tube furnace. The ampoule had an estimated gas-to-melt volume sufficiently large to secure an excess of SO₂ even after complete reduction to V(III) of the vanadium present. A bright green solution (indicating a high degree of vanadium reduction) was obtained within few hours. The temperature was then reduced gradually to 370°C, when small crystals appeared, and afterwards it was lowered to 320°C in steps of 5–10°C during a period of one week. This resulted in the formation of a large amount of small dark-green crystals, accompanied by a decoloration of the melt, indicating that almost all vanadium had precipitated.

The crystals were isolated by cutting the ampoule open and gently flushing the solidified content with water, which resulted in dissolution of NaHSO₄. Proper crystals, suitable for X-ray analysis, were isolated under a polarization microscope.

It is noteworthy how the solvent and gas composition influences the compound formation. Thus, blue needle-shaped crystals of the V⁴⁺ compound Na₂VO(SO₄)₂^{2,5} are precipitated while V₂O₅-Na₂S₂O₇ (Na/V = 3–5) melts are treated with a 10% SO₂, 11% O₂, 79% N₂ mixture in a reactor flow cell in the temperature range 470–400°C. On the other hand, only green crystals were obtained from V₂O₅-Na₂S₂O₇ melts with the molar ratio Na/V = 4 treated with a 10% SO₂, 90% N₂ gas mixture at 470°C. Surprisingly, these crystals consisting mainly of another V⁴⁺ compound [(Na₈(VO)₂(SO₄)₆] as identified by a single-crystal X-ray investigation¹⁰ were green [V(IV) compounds are usually blue], while a small amount of the green NaV(SO₄)₂⁶ was also isolated. Furthermore, equilibrating a V₂O₅-Na₂S₂O₇ (Na/V = 4.7) molten mixture under 0.9 atm SO₂ in a sealed ampoule in the temperature range 450–400°C resulted in the formation of NaV(SO₄)₂ only.

Infrared spectra. IR spectra were recorded on a BOMEM DA3.26 FITR spectrometer. The samples were ground in dry KBr and pressed into transparent discs.

Raman spectra. Raman spectra of polycrystalline samples were excited with the 514.5 and 488.0 nm lines of a 4 W

Spectra Physics argon ion laser. The scattered light was collected at an angle of 90° (horizontal scattering plane) and analyzed with a Spex 1403 0.85 m double monochromator equipped with a -20°C-cooled RCA photomultiplier and EG&G/ORTEC photon counting electronics. Samples contained in sealed tubes were immersed in liquid nitrogen in order to obtain spectra at 77 K.

X-Ray investigation. Crystal data for Na₃V(SO₄)₃ are given in Table 1. The intensity data were collected on an Enraf-Nonius CAD-4F diffractometer with monochromated MoK α radiation. The cell dimensions were determined by least-squares refinement based on the settings of 25 high-order reflections. The intensity data were corrected for Lorentz and polarization effects and corrected for absorption by an empirical method,¹¹ in which the crystal shape is approximated by an ellipsoid and the size (in units of μm^{-1}) and orientation are treated as parameters. The refinement of the six parameters is based on ψ -scans, in the present case ψ -scans on four reflections and all their symmetry-related reflections. The quantity minimized was $R = \sum w(I_{\text{obs}} - I_{\text{corr}}A)^2$, where A is the absorption coefficient. The minimization problem consisted of 411 observations and 6 parameters and was accomplished via the SIMPLEX method.¹² The initial and final values of $R_w = (R/\sum wI_{\text{obs}}^2)^{1/2}$ are 0.0390 and 0.0166, respectively. An estimate of the linear absorption coefficient, μ , may be found as the cube root of the ratio between the volume of the ellipsoid and the (approximate) volume of the crystal. A value of 24 cm⁻¹ was obtained, in fair agreement with the actual value of 18.46 cm⁻¹. The minimum and maximum transmission coefficients are 0.6601 and 0.7795, respectively.

The structure was solved by Patterson and Fourier techniques and the structural parameters were refined by full-matrix least-squares methods.¹³ The atomic scattering factors and the anomalous dispersion corrections

Table 1. Crystal data for Na₃V(SO₄)₃.

$M_w/\text{g mol}^{-1}$	408.095
Crystal system	Rhombohedral (hexagonal setting)
Space group	$R\bar{3}$
$a/\text{\AA}$	13.439(1)
$c/\text{\AA}$	9.091(1)
Z	6
$V/\text{\AA}^3$	1421.92
$D_c/\text{g cm}^{-3}$	2.860
$\mu(\text{MoK}\alpha)$	18.46
Crystal size/mm	0.19 × 0.15 × 0.09
$\theta_{\text{max}}/^\circ$	40
Total no. of reflections	3154
No. of unique reflections	1954
R between symmetry-related reflections $[\sum w(I - \langle I \rangle)^2 / \sum wI^2]^{1/2}$	0.0194
No. of rejected reflections	310
No. of parameters	59
Weight function, w	$w^{-1} = \sigma^2(F) + 0.0003F^2$
$R_1 = \sum \ F_o\ - F_c / \sum F_o $	0.0274
$R_2 = (\sum w(F_o - F_c)^2 / \sum w F_o ^2)^{1/2}$	0.0399

Table 2. Coordinates of the atoms in $\text{Na}_3\text{V}(\text{SO}_4)_3$.^a

Atom	x/a	y/b	z/c	U_{eq}^b
V(1)	0	0	0	0.0092
V(2)	0	0	0.5	0.0080
S	-0.0251(1)	0.1623(1)	0.2599(1)	0.0095
Na	-0.2557(1)	0.1079(1)	-0.5086(1)	0.0273
O(1)	0.0338(1)	0.1366(1)	0.3801(1)	0.0208
O(2)	-0.1480(1)	0.1016(1)	-0.7198(1)	0.0207
O(3)	0.0284(1)	0.2871(1)	-0.7427(1)	0.0188
O(4)	0.0070(1)	0.1291(1)	0.1182(1)	0.0234

^aThe temperature factor parameters can be obtained from the authors. ^b $U_{\text{eq}} = 1/3 \sum U_{ij} a_i^* a_j^* a_i a_j$.

are from Ref. 14. Details of the refinement are given in Table 1. Atomic coordinates, equivalent isotropic parameters, bond lengths and angles are listed in Tables 2 and 3. Lists of observed and calculated structure factors as well as anisotropic thermal parameters may be obtained from the authors.

Results and discussion

Description of the structure. The unit cell contains two crystallographically independent VO_6 octahedra with the vanadium atoms situated on three-fold inversion axes, e.g. (0, 0, 0) and (0, 0, $1/2$). The VO_6 units are almost perfect octahedra. Identical V–O bond lengths are found within each octahedron. All oxygens coordinated to vanadium are sulfate oxygens [O(4) and O(1)] but there are also oxygens, i.e. O(2) and O(3), which are bound to sulfur but not to vanadium. As shown in Fig. 1, the crystallographically different vanadium atoms are linked by three bridging sulfate groups, thus forming an infinite chain parallel to the *c*-axis. The remaining two sulfate oxygens have short contact distances to the sodium ion, which are located between the $-\text{V}-(\text{SO}_4)_3-\text{V}-$ chains. Bond distances and angles for the octahedra are given in Table 3 and have values typical of vanadium(III) compounds.¹⁵

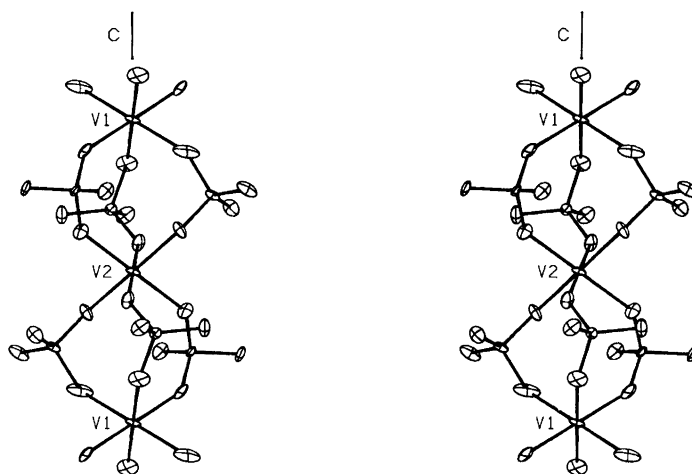


Fig. 1. Stereo plot of the infinite $-\text{V}-(\text{SO}_4)_3-\text{V}-$ chain along the *c*-axis.

Table 3. Bond and contact lengths (in Å) and angles (in °) in $\text{Na}_3\text{V}(\text{SO}_4)_3$.^a

V(1)–O(4)	2.003 (6×)	O(4)–V(1)–O(4)	180 (3×)
			93.9 (6×)
			86.1 (6×)
V(2)–O(1)	1.982 (6×)	O(1)–V(2)–O(1)	180 (3×)
			92.6 (6×)
			87.4 (6×)
S–O(2)	1.442	O(2)–S–O(3)	114.9
S–O(3)	1.457	O(2)–S–O(1)	111.5
S–O(1)	1.489	O(2)–S–O(4)	111.2
S–O(4)	1.496	O(3)–S–O(1)	105.4
		O(3)–S–O(4)	106.2
		O(1)–S–O(4)	107.2
Na–O(3)	2.294, 2.514, 2.702		
Na–O(2)	2.431, 2.521		
Na–O(4)	2.711		
Na–O(1)	2.938		

^aESD: 0.001 Å for lengths and 0.1° for angles.

The bond lengths between sulfur and non-coordinated oxygens [O(2) and O(3)] are relatively short (1.442 and 1.457 Å) compared with the S–O(4) and S–O(1) bonds (1.489 and 1.496 Å) found in the vanadium–oxygen–sulfur coordination bridges. Around the sulfur atoms, nearly tetrahedral angles are found deformed in such a way that the bridging O(1)–S–O(4) angles (107.2°) are smaller than the ideal tetrahedral angle of 109.47°, probably due to repulsion from the short-bonded oxygens, whereas the O(2)–S–O(3) angles of 114.9° involving the non-coordinated oxygens are larger than 82 out of 84 measured O–S–O angles in the sulfate groups of six different vanadium compounds $\text{K}_4(\text{VO})_3(\text{SO}_4)_5$, $\text{KV}(\text{SO}_4)_2$, $\text{Na}_2\text{VO}(\text{SO}_4)_2$, $\text{NaV}(\text{SO}_4)_2$, $\text{CsV}(\text{SO}_4)_2$ and $\text{Cs}_4(\text{VO})_2\text{O}(\text{SO}_4)_4$.^{3–6,8,16} Generally, the S–O distances were found to depend on the angles in such a way that the larger the average of the three possible O–S–O angles involving a particular bond, the smaller is the S–O distance of that bond. This is shown in Fig. 2, where an approximately linear relationship (linear regression) is found which is similar to that observed for the twelve

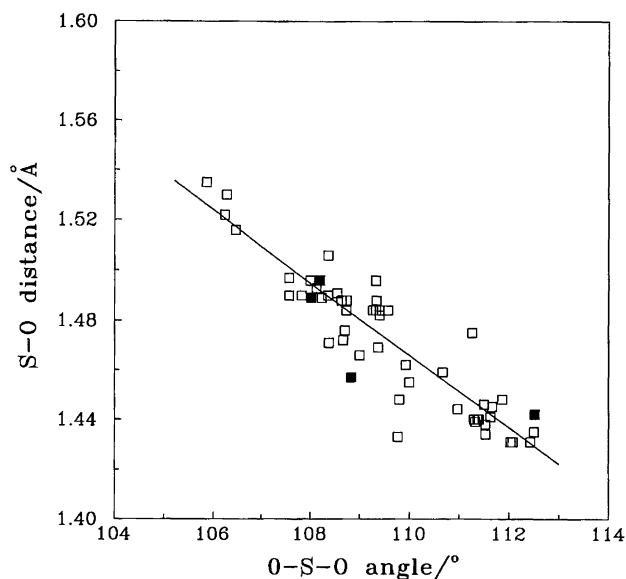


Fig. 2. Plot of S-O distances for a particular bond versus the average of the three angles involving this bond and the other S-O bonds of the sulfate tetrahedron (four solid points). Also shown are 49 points from the literature.^{3-6,8,16}

different sulfate ions in the $\text{K}_4(\text{VO})_3(\text{SO}_4)_5$, $\text{KV}(\text{SO}_4)_2$, $\text{Na}_2\text{VO}(\text{SO}_4)_2$, $\text{NaV}(\text{SO}_4)_2$, $\text{CsV}(\text{SO}_4)_2$ and $\text{Cs}_4(\text{VO})_2\text{O}(\text{SO}_4)_4$ structures.^{3-6,8,16} This dependence indicates a general relationship between S-O bond distances and hybridization of the sulfur atom in the sulfate groups in these cases as pointed out previously,³ except for a possible partial breakdown in the case of $\text{Cs}_4(\text{VO})_2\text{O}(\text{SO}_4)_4$.¹⁶ Generally, the bond lengths and bond angles of the sulfate tetrahedra (Table 3) are close to the usual values of 1.474 Å and 109.47° for the sulfate group.¹⁷

Vibrational spectra. Oriented single-crystal vibrational spectroscopic work using polarized light was difficult to undertake because of the large crystal unit cell of $\text{Na}_3\text{V}(\text{SO}_4)_3$ and the polyhedral crystal shape. Therefore, only powder work is reported. Vibrational spectra of the $\text{NaV}(\text{SO}_4)_2$ compound, previously characterized by single crystal X-ray analysis,⁶ were also obtained and are reported in this work.

If the $\text{Na}_3\text{V}(\text{SO}_4)_3$ crystal is considered to be composed of Na^+ , V^{3+} and SO_4^{2-} ions, one should expect to observe the free group vibrations of the complex ion (here SO_4^{2-}), i.e. a number of bands near the positions of the four SO_4^{2-} fundamentals that are known to span the following representation for a regular tetrahedral (T_d) ion configuration:

$$\Gamma_{\text{vib}} = A_1(\nu_1) + E_2(\nu_2) + 2F_2(\nu_3 + \nu_4)$$

All modes are Raman active and only F_2 is IR allowed. In the usual approximation of weak couplings, modes labelled as ν_1 and ν_3 are stretchings and ν_2 and ν_4 are bendings. In $\text{Na}_3\text{V}(\text{SO}_4)_3$, the equivalent SO_4^{2-} ions

present in the unit cell have nine internal vibrational degrees of freedom that should be distributed on the original ν_1 - ν_4 sulfate modes that are well known,¹⁸ mainly from Raman spectroscopy on aqueous sulfate solutions: $\nu_1(A_1) \approx 981 \text{ cm}^{-1}$, $\nu_2(E) \approx 451 \text{ cm}^{-1}$, $\nu_3(F_2) \approx 1104 \text{ cm}^{-1}$ and $\nu_4(F_2) \approx 613 \text{ cm}^{-1}$. Infrared spectra of a large number of hexagonal ($P 321$) $M^{\text{I}}M^{\text{III}}(\text{SO}_4)_2$ salts in KBr disks have previously been recorded and assigned,^{19,20} and thorough vibrational analyses, including oriented single-crystal Raman work on $\text{KV}(\text{SO}_4)_2$ ⁴ and $\text{CsV}(\text{SO}_4)_2$,⁸ have been performed.

Infrared spectra. Figure 3 shows infrared spectra of dark green $\text{Na}_3\text{V}(\text{SO}_4)_3$ and bright green $\text{NaV}(\text{SO}_4)_2$ obtained at room temperature from finely ground powders in pressed KBr disks. The IR band positions for both compounds are summarized in Table 4.

Raman spectra. Raman spectra obtained from stationary polycrystalline $\text{Na}_3\text{V}(\text{SO}_4)_3$ and $\text{NaV}(\text{SO}_4)_2$ samples at room temperature are shown in Figs. 4 and 5, respectively. Both the 514.5 nm and the 488.0 nm argon laser lines were used to excite spectra without significant differences in the exhibited spectral features. Spectra were recorded also at liquid nitrogen temperature, and apart from the expected effect of band sharpening were identical with those recorded at room temperature in terms of numbers and positions of bands observed. The Raman wavenumbers are listed in Table 4.

Discussion. The infrared bands observed in the IR spectra of both the $\text{Na}_3\text{V}(\text{SO}_4)_3$ and $\text{NaV}(\text{SO}_4)_2$ compounds

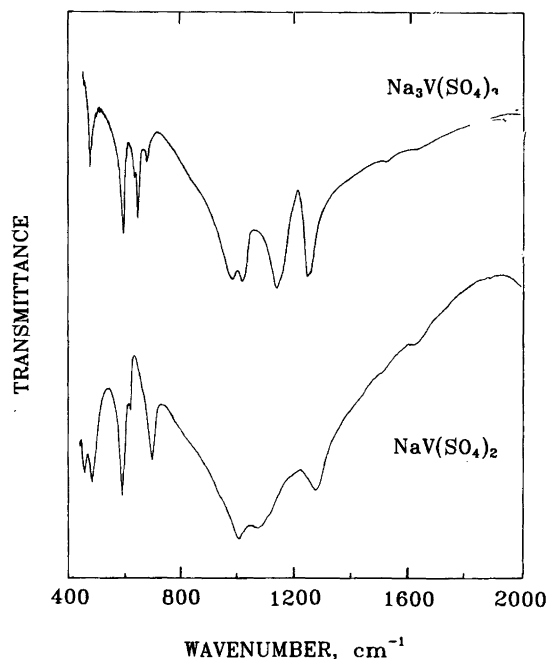


Fig. 3. Infrared spectra of $\text{Na}_3\text{V}(\text{SO}_4)_3$ and $\text{NaV}(\text{SO}_4)_2$ powders in pressed KBr disks at room temperature. Resolution, ca. 5 cm^{-1} .

Table 4. Infrared and Raman bands (cm^{-1}) of $\text{Na}_3\text{V}(\text{SO}_4)_3$ and $\text{NaV}(\text{SO}_4)_2$ and their tentative assignments.^a

$\text{Na}_3\text{V}(\text{SO}_4)_3$			$\text{NaV}(\text{SO}_4)_2$		
IR (Fig. 3)	Raman (Fig. 4)	Assignment	IR (Fig. 3)	Raman (Fig. 5)	Assignment
	~ 1590 w,vbr	$\nu_e, ({}^3E_g \leftarrow {}^3A_g)^b$		~ 1610 w,vbr	$\nu_e, ({}^3E_g \leftarrow {}^3A_g)$
1256 w,sh	1300 m	ν_3		1305 s	ν_3
1245 s	1254 m	ν_3	1276 m		ν_3
	1198 m	ν_3	1112 w,sh	1114 w,sh	
1136 s		ν_3	1074 s	1065 s	ν_3
1018 s		ν_3	1002 s	1008 s	ν_3
981 s	1036 vs	ν_1	940 w,sh	933 vs	ν_1
	962 m,br	$2\nu_2(478)?$		~ 1000 m,br	$2\nu_2(495)?$
665 w		ν_4	698 s	685 w	ν_4
641 s	641 m	ν_4	624 w		ν_4
632 w,sh					
592 s	593 m	ν_4	592 s	598 m	ν_4
477 s	478 m	ν_2	487 m	495 m	ν_2
	443 m	ν_2^c	458 w	457 m	ν_2
	290 m	ν_L^c		315 s	ν_L
	221 m,sh	ν_L		223 m	ν_L
	146 sh	ν_L		141 vs	ν_L

^aIntensity codes: w: weak; m: medium; s: strong; v: very; br: broad; sh: shoulder. ^b ν_e : electronic mode. ^c ν_L : lattice mode.

(Fig. 3) can be assigned unambiguously as due to the ν_1 – ν_4 sulfate ion fundamentals (Table 4). As can be seen from Figs. 3–5 many of the observed bands are common to both kinds of spectra for each of the examined compounds. The presence in the IR and Raman spectra of a number of bands in the regions of 1000–1300, 600–700 and 450 – 500 cm^{-1} is interpreted as indicating a lowering of the T_d symmetry of the free SO_4^{2-} group in both $\text{Na}_3\text{V}(\text{SO}_4)_3$ and $\text{NaV}(\text{SO}_4)_2$ crystals. Coordination of the sulfate ion and interactions with other ions in the crystal lattice is indeed known to reduce the symmetry and lift the degeneracies of the ν_2 , ν_3 and ν_4 modes.¹⁸ Similar band-rich spectra were reported for

$\text{Na}_2\text{VO}(\text{SO}_4)_2$,⁵ $\text{k}_2(\text{VO})_3(\text{SO}_4)_5$ ³ and for sulfate groups studied under various crystal environments.²¹

A careful examination of the Raman spectra indicates that most bands can be easily and unambiguously assigned as due to ν_1 – ν_4 (sulfate) and ν_L (lattice) modes (Table 4). However, the spectra of both compounds contain features that call for further attention. Firstly, as shown in Figs. 4 and 5, Raman spectra of both $\text{Na}_3\text{V}(\text{SO}_4)_3$ and $\text{NaV}(\text{SO}_4)_2$ exhibit a very broad weak band centred around ca. 1600 cm^{-1} , i.e. ca. 300 cm^{-1} further away from the most blue-shifted ν_3 component. Secondly, both spectra possess a broad band of appre-

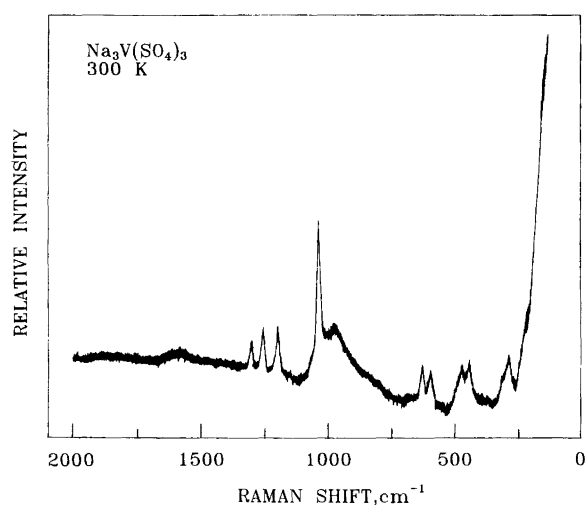


Fig. 4. Raman spectrum of $\text{Na}_3\text{V}(\text{SO}_4)_3$ powder at room temperature. $\lambda_0 = 514.5\text{ nm}$; laser power, 200 mW; resolution, ca. 2 cm^{-1} .

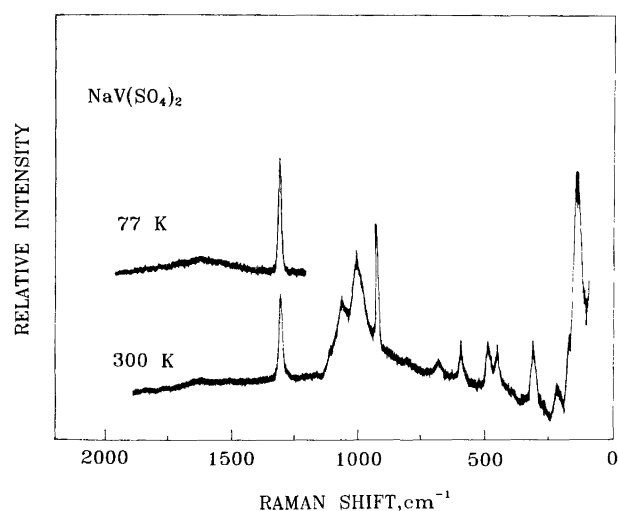


Fig. 5. Raman spectrum of $\text{NaV}(\text{SO}_4)_2$ powder at room temperature. Insert shows the high frequency range at liquid nitrogen temperature. $\lambda_0 = 514.5\text{ nm}$; laser power, 200 mW; resolution, ca. 2 cm^{-1} .

ciable intensity, located at 962 cm⁻¹ for Na₃V(SO₄)₃ and ca. 1000 cm⁻¹ for NaV(SO₄)₂, the latter band being obscured by the 933 (ν₁), 1008 (ν₃) and 1065 (ν₃) modes.

The broad weak bands around 1600 cm⁻¹ are attributed to electronic Raman transitions of the V³⁺ ion. A characteristic feature of electronic Raman bands is that they are generally much broader than vibrational bands, even at very low temperatures.^{22,23} Spectra of samples from different preparations, using different excitation laser lines (i.e. 488.0 and 514.5 nm), preclude the assignment of these bands either to an impurity or as resulting from a fluorescent process.

It should be pointed out that electronic Raman transitions of the V³⁺ ion have been observed previously in the KV(SO₄)₂⁴ and CsV(SO₄)₂⁸ crystals at ca. 1560 and ca. 1400 cm⁻¹ respectively and in the CsV(SO₄)₂·12H₂O and NH₄V(SO₄)₂·12H₂O compounds at ca. 1940 cm⁻¹.²⁴

As discussed in the reports on CsV(SO₄)₂⁸ and KV(SO₄)₂,⁴ the ground electronic state of V³⁺ (d²) in octahedral field is ³T_{1g}(³F), which in a trigonal S₆ field splits into a ³E_g and a ³A_g state.^{25,26} It is normally assumed that the ³A_g state is the ground state. Similar splittings occur in the two excited triplet states ³T_{2g}(³F) and ³T_{1g}(³P). In Fig. 6 the electronic states of V³⁺ in octahedral oxide fields are estimated by using a theoretical energy diagram²⁶ with the Dq parameter being ca. 1600 cm⁻¹. In

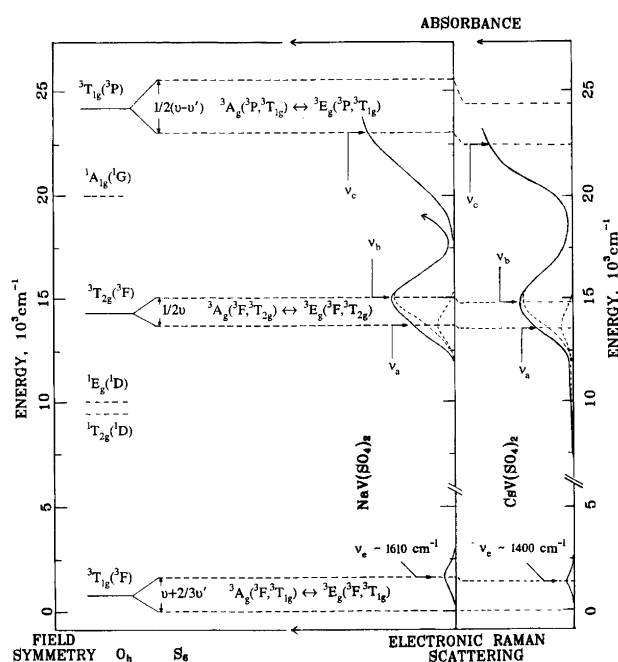


Fig. 6. Energy states of V³⁺ with $Dq \approx 1600$ cm⁻¹ in an octahedral O_h field and splittings of triplet states in the trigonal field of NaV(SO₄)₂. O_h energy states underlined by broken lines indicate states associated with spin-forbidden transitions from the ground state. The absorption (ν_a, ν_b and ν_c) and electronic Raman (ν_e) bands of crystalline NaV(SO₄)₂ are shown in arbitrary intensity units. To the right, the respective spectra of crystalline CsV(SO₄)₂ are included for comparison.

the same figure the visible absorption spectrum of crystalline NaV(SO₄)₂ is presented, and the respective spectrum of CsV(SO₄)₂⁸ is also included for comparison. The Na₃V(SO₄)₃ that usually grows in polyhedral shaped crystals did not allow the recording of a similar spectrum for this compound. Nevertheless, the V³⁺ energy levels are not expected to be significantly different, as can be seen by comparing the electronic spectra of CsV(SO₄)₂⁸ and KV(SO₄)₂.⁴ The observed bands in the visible region are attributed to transitions of V³⁺ in the trigonal crystal field:

$${}^3A_g({}^3F, {}^3T_{2g}) \leftarrow {}^3A_g({}^3F, {}^3T_{1g}), \quad \nu_a \approx 13\,600 \text{ cm}^{-1}$$

$${}^3E_g({}^3F, {}^3T_{2g}) \leftarrow {}^3A_g({}^3F, {}^3T_{1g}), \quad \nu_b \approx 15\,100 \text{ cm}^{-1}$$

These values are obtained by resolving the broad feature centred at ca. 14900 cm⁻¹ into Gaussians. The deconvolution is made by assuming that the relative intensities of the two bands are the same as in the case of CsV(SO₄)₂⁸ and KV(SO₄)₂.⁴ The shoulder band in the near UV region is assigned to the split component, ³A_g, of the second triplet excited state ³T_{1g}(³P):

$${}^3A_g({}^3P, {}^3T_{1g}) \leftarrow {}^3A_g({}^3F, {}^3T_{1g}), \quad \nu_c \approx 23\,000 \text{ cm}^{-1}$$

The separation of the ³A_g(³T_{2g}) and ³E_g(³T_{2g}) states is $\Delta\nu = \nu_b - \nu_a \approx 1500$ cm⁻¹, which according to ligand field calculations^{25,26} is smaller than the separation of the ³E_g(³T_{1g}) and ³A_g(³T_{1g}) in the ground state. In other words, for the V³⁺ ion in the NaV(SO₄)₂ and Na₃V(SO₄)₃ crystals, the first electronic Raman transitions are likely to occur in a region near and above 1500 cm⁻¹. The broad weak bands at ca. 1590 and ca. 1610 cm⁻¹ in the Raman spectra of Na₃V(SO₄)₃ and NaV(SO₄)₂ are in this expected region and are thus assigned to the electronic transitions between the split components of the ground state, ³T_{1g}(³F). Such a transition is allowed according to the electronic Raman selection rules, since the direct product A_g × E_g contains the representation E_g which belongs to the Raman polarizability tensor components.^{22,23}

On the basis of crystal-field model calculations, the splitting of octahedral states in trigonal fields of intermediate strength can be calculated in terms of two parameters ν and ν'.²⁵⁻²⁷ For the triplet states in Fig. 6 the splittings are:

$$\Delta[{}^3T_{1g}({}^3F)] = \nu + 2/3\nu'$$

$$\Delta[{}^3T_{2g}({}^3F)] = 1/2\nu$$

$$\Delta[{}^3T_{1g}({}^3P)] = 1/2(\nu - \nu')$$

The values of the first two splittings measured from the spectra of NaV(SO₄)₂ are ca. 1610 and ca. 1500 cm⁻¹ respectively, and thus $\nu \approx 3000$ cm⁻¹ and $\nu' \approx -2085$ cm⁻¹. From the third difference, the energy of the upper ³E_g(³P, ³T_{1g}) state can be estimated as ca. 25500 cm⁻¹, based on $\nu_c \approx 23000$ cm⁻¹.

Table 5 lists the electronic Raman transitions observed to date between the 3E_g and 3A_g split components of the ${}^3T_{1g}({}^3F)$ ground state of V^{3+} in octahedral oxide fields.

As mentioned above, the Raman spectra in Figs. 4 and 5 also show broad bands in the spectral range around 1000 cm^{-1} [i.e. 962 cm^{-1} for $\text{Na}_3\text{V}(\text{SO}_4)_3$ and ca. 1000 cm^{-1} for $\text{NaV}(\text{SO}_4)_2$]. Similar bands are exhibited in the crystal Raman spectra of $\text{KV}(\text{SO}_4)_2$ and $\text{CsV}(\text{SO}_4)_2$ at ca. 950 and 924 cm^{-1} , respectively. The origin of these bands is not yet completely understood. As shown in Fig. 6 the green-to-blue laser lines used to excite the Raman spectra overlap with the tail of the Laporteforbidden UV absorption bands corresponding to transitions from the ground state to the ${}^3A_g({}^3P, {}^3T_{1g})$ and ${}^3E_g({}^3P, {}^3T_{1g})$ levels. Therefore, the electronic and vibrational Raman bands might exhibit preresonance enhancement of their intensities,²³ and a series of combinations and/or overtones of fundamental vibrations might be observed in the Raman spectrum. Consequently, the 962 and ca. 1000 cm^{-1} bands can be due to a combination or an overtone of lower-lying fundamentals, whose intensity enhancement could be accounted for by the preresonance conditions described or by Fermi resonance with the ν_1 mode. For example, the first overtones of the ν_2 modes at 478 for $\text{Na}_3\text{V}(\text{SO}_4)_3$ and 495 cm^{-1} for $\text{NaV}(\text{SO}_4)_2$ result in states with energies at 956 and 990 cm^{-1} , which are lying very close to the observed 962 and ca. 1000 cm^{-1} bands. As pointed out by one of the reviewers, use of excitation sources with energies lying far away from the energies of the electronic transitions (e.g. recording the NIR-FT Raman spectra of the compounds) can provide conclusive evidence concerning whether the intensity increase of the overtones is due to preresonance conditions or not. The broad bands previously observed at 950 and 924 cm^{-1} in the crystal Raman spectra of $\text{KV}(\text{SO}_4)_2$ and $\text{CsV}(\text{SO}_4)_2$ can also be attributed to the first overtones of the respective $\nu_2(E_g)$ modes observed at 474 and 467 cm^{-1} , respectively.^{4,8} It seems less likely that the 962 and ca. 1000 cm^{-1} bands (Table 4) could be of electronic origin. Electronic Raman transitions are generally very weak, and it is not expected that a resonance between a totally symmetric vibrational state [i.e. $\nu_1(\text{SO}_4^{2-})$] and an electronic state can transfer appreciable intensity from the vibrational to the electronic band.

Table 5. Energies of electronic Raman transitions, ν_e , between the 3E_g and 3A_g split components of the ${}^3T_{1g}({}^3F)$ ground state of $V^{3+}(d^2)$ in octahedral oxide crystal fields.

Crystal	$\nu_e\text{ cm}^{-1}$	Ref.
$\text{Na}_3\text{V}(\text{SO}_4)_3$	~ 1590	(This work)
$\text{NaV}(\text{SO}_4)_2$	~ 1610	(This work)
$\text{KV}(\text{SO}_4)_2$	~ 1560	4
$\text{CsV}(\text{SO}_4)_2$	~ 1400	8
$\text{CsV}(\text{SO}_4)_2 \cdot 12\text{H}_2\text{O}$	~ 1940	23
$\text{NH}_4\text{V}(\text{SO}_4)_2 \cdot 12\text{H}_2\text{O}$	~ 1940	23

Conclusions

The compound $\text{Na}_3\text{V}(\text{SO}_4)_3$ has been isolated from $\text{NaHSO}_4/\text{V}_2\text{O}_5$ under an SO_2 atmosphere and its structure was determined. The infrared and Raman spectra of polycrystalline $\text{Na}_3\text{V}(\text{SO}_4)_3$ and of $\text{NaV}(\text{SO}_4)_2$ have been recorded and interpreted. The severe distortion of the sulfate groups within $\text{Na}_3\text{V}(\text{SO}_4)_3$ leads to a more complicated pattern of the vibrational spectra [i.e. IR activity of $\nu_1(\text{SO}_4^{2-})$ and extensive splitting of $\nu_3(\text{SO}_4^{2-})$ in the IR and Raman spectra] compared to $\text{NaV}(\text{SO}_4)_2$. This is in good accordance with the sulfur-oxygen bond lengths, interionic distances and geometries of distorted sulfate groups found in $\text{Na}_3\text{V}(\text{SO}_4)_3$ (Table 3) and $\text{NaV}(\text{SO}_4)_2$.⁶ Above 1500 cm^{-1} the Raman spectra, particularly at lower temperatures, exhibit broad features which are interpreted as electronic Raman transitions between the 3E_g and 3A_g split levels of the ${}^3T_{1g}({}^3F)$ ground state of $V^{3+}(d^2)$ in octahedral oxide fields.

Acknowledgments. This investigation has been supported by the EEC BRITE-EURAM II (contract no. BRE2.CT93.0447) and Human Capital and Mobility (contract no. ERBCHBG.CT92.029) programmes. Support from the Danish Natural Science Research Council is acknowledged. We are indebted to Professor George Papatheodorou for helpful discussions and valuable comments.

References

- Villadsen, J. and Livbjerg, H. *Catal. Rev.-Sci. Eng.* 17 (1978) 203.
- Boghosian, S., Fehrmann, R., Bjerrum, N. J., Papatheodorou, G. N. *J. Catal.* 119 (1989) 121.
- Fehrmann, R., Boghosian, S., Papatheodorou, G. N., Nielsen, K., Berg, R. W. and Bjerrum, N. J. *Inorg. Chem.* 28 (1989) 1847.
- Fehrmann, R., Krebs, B., Papatheodorou, G. N., Berg, R. W. and Bjerrum, N. J. *Inorg. Chem.* 25 (1986) 1571.
- Fehrmann, R., Boghosian, S., Papatheodorou, G. N., Nielsen, K., Berg, R. W. and Bjerrum, N. J. *Inorg. Chem.* 29 (1990) 3294.
- Fehrmann, R., Boghosian, S., Papatheodorou, G. N., Nielsen, K., Berg, R. W. and Bjerrum, N. J. *Acta Chem. Scand.* 45 (1991) 961.
- Boghosian, S., Nielsen, K., Fehrmann, R. and Berg, R. W. *To be submitted.*
- Berg, R. W., Boghosian, S., Bjerrum, N. J., Fehrmann, R., Krebs, B., Sträter, N., Mortensen, O. S. and Papatheodorou, G. N. *Inorg. Chem.* 32 (1993) 4714.
- Eriksen, K. M., Fehrmann, R. and Bjerrum, N. J. *J. Catal.* 132 (1991) 263.
- Nielsen, K., Boghosian, S. and Fehrmann, R. *To be submitted.*
- Nielsen, K. *To be published.*
- Nelder, J. A. and Mead, R. *Comput. J.* 7 (1964-65) 308.
- Sheldrick, G. M. *SHELX-76 Program for Crystal Structure Determination*, University of Göttingen, FRG 1976.
- International Tables for X-ray Crystallography*, Vol. IV, Kynoch Press, Birmingham 1974.
- Selbin, J. *Coord. Chem. Rev.* 1 (1966) 293; *Chem. Rev.* 65 (1965) 153.

16. Nielsen, K., Fehrmann, R. and Eriksen, K. M. *Inorg. Chem.* 32 (1993) 4825.
17. Renner, B. and Lehmann, G. Z. *Kristallogr., Kristallgeom., Kristallphys., Kristallchem.* 175 (1986) 43.
18. Nakamoto, K. *Infrared and Raman Spectra of Inorganic Coordination Compounds*, Wiley, New York 1978.
19. Couchot, P., Mercier, R. and Bernard, J. *Bull. Soc. Chim. Fr.* (1970) 3433.
20. Couchot, P., Nguyen Minh Hoang, F. and Perret, R. *Bull. Soc. Chim. Fr.* (1971) 360.
21. Bremard, C., Laureyns, J. and Abraham, F. *J. Raman Spectrosc.* 17 (1986) 397.
22. Koningstein, J. A. *Mol. Spectrosc.* 4 (1976) 196; Koningstein, J. A. *Vib. Spectra Struct.* 9 (1981) 115.
23. Clark, R. J. H. and Dines, T. J. *Adv. Infrared Raman Spectrosc.* 9 (1982) 282.
24. Best, S. P. and Clark, R. J. H. *Chem. Phys. Lett.* 122 (1985) 401.
25. Hush, N. S. and Hobbs, R. J. M. *Progr. Inorg. Chem.* 10 (1968) 259.
26. Ferguson, J. *Progr. Inorg. Chem.* 12 (1970) 159.
27. Macfarlane, R. M. *J. Chem. Phys.* 40 (1964) 373.

Received February 21, 1994.